Special Feature: Advanced Thermal Management Technology for Developing the High-efficiency Vehicle

Research Report

A Study on Thermal Conductivity Increase in Nanofluids

Kazuhisa Yano and Koji Yoshida

Report received on Jun. 11, 2018

ABSTRACT Increases in the thermal conductivities of liquids containing low concentrations of nanoparticles (so-called nanofluids) were examined using inelastic X-ray scattering. Assessments of coherent scattering from nanofluid solvents were employed to determine the high-frequency sound velocity. Both the structural relaxation and thermal conductivity of solvent molecules affect the sound velocity, and so these data allowed an analysis of modifications of molecular dynamics and heat transport due to the addition of nanoparticles. Significant increases in sound velocity in ethylene glycol were obtained with Cu nanoparticles, although alumina NPs in water had a minimal effect. Sound velocity variations were also found to closely correlate with thermal conductivity values. These results demonstrate that the Cu nanoparticles increased the thermal conductivity by greatly restraining the solvent molecules in the nanofluid.

KEYWORDS Thermal Conductivity, Nanofluids, Collective Dynamics, Inelastic X-ray Scattering, High-frequency Sound Velocity

1. Introduction

The field of thermal management has been the subject of much research, including investigations of subjects including heat transport, energy conversion and thermal storage. The usage of waste heat has attracted significant attention, particularly in the automobile industry, since 60 to 70% of the energy in automotive fuel is lost as waste heat. Greater fuel efficiency could be obtained by employing this waste heat, but high-efficiency heat transfer media are needed to convey this heat to units for heat storage or conversion. Another issue associated with waste heat is the large radiator size required for fuel cell automobiles (to dissipate the large amount of heat generated by the reaction in the cell), which limits the minimum size of such vehicles. Both these issues could be addressed by the development of new heat transfer media.

The availability of new fluids with greater thermal conductivity could lead to more efficient heat transfer media, and there has been much work concerning nanoparticle (NP) dispersions in liquids to produce so-called nanofluids.[1-7] As an example, adding Ag, Cu or alumina NPs in small quantities raises the thermal conductivity of various liquids, including ethylene glycol (EG), gear oil and water, by 20 to 40%.[8] Clustering, Brownian motion, inter-NP potential and ballistic transport could all be associated with the increased thermal conductivities of nanofluids.[9] As an example, dynamic light scattering and transmission electron microscopy observations have provided evidence for clustering.[10] Despite this, there have not yet been detailed investigations of the interactions between NPs and solvents, even though such research would assist in the design of high-efficiency heat transfer media.

The collective dynamics of water,[11,12] organic solvents,[13,14] liquid metals[15-17] and other fluids have been examined by high resolution inelastic X-ray scattering (IXS). Using this technique, the coherent scattering from nanofluids can be employed to assess the solvent molecule collective dynamics. At low momentum transfer values (from 2 to 20 nm^{-1}), the collective dynamics are reflected in the excitation of acoustic phonons. For this reason, the relationship between the excitation energy and momentum transfer

can be used to estimate the high frequency sound velocity. This velocity is affected by the solvent structural relaxation and thermal conductivity, allowing an analysis of the manner in which molecular dynamics and heat transfer are affected by the addition of NPs.

In the present study, the polyol method was employed to synthesize Cu NPs having an average diameter of 50 nm.[18-21] These NPs were purposely fabricated with a narrow particle size distribution because thermal conductivity has been found to correlate strongly with NP size.[22] Nanofluid specimens were produced based on loading EG with Cu NPs, after which both IXS and thermal conductivity analyses were performed. A second nanofluid based on water containing alumina NPs was also employed, for comparison purposes. The data demonstrate that the thermal conductivity of the nanofluid is increased by the addition of Cu NPs as a result of the effect of these NPs on the solvent molecules.

2. Methods

2. 1 Materials

Cu NPs were synthesized according to a procedure in the literature,[21] but using polyvinylpyrrolidone (PVP) as a stabilizer instead of dodecanoic acid and dodecyl amine. The average particle diameter was determined to be approximately 60 nm (with a standard deviation of 15%) based on a transmission electron microscopy (TEM) image. These Cu NPs were added to EG and sonicated to obtain a dispersion. Alumina (average particle size approximately 30 nm) in water dispersions with alumina concentrations of 10 and 30 wt% were obtained from CI Kasei Co., Ltd.

2. 2 Nanofluid Characterization

The concentration of Cu NPs in each nanofluid was estimated from thermogravimetric analysis (TGA) in air using an LFA447 NANOFLASH (NETZSCH). Aliquots of each liquid were transferred into a cell made of Pt/Rh, 12 mm in diameter and 0.29 mm thick, and covered with a 0.3 mm thick lid such that the liquid sample was 0.53 nm thick. The thermal conductivity of the resulting layered structure was measured by the laser flash method and the thermal conductivity of the liquid sample was subsequently calculated.

2. 3 IXS Experiments

The IXS analyses were carried out using the high-resolution IXS spectrometer installed at the BL35XU beamline at the SPring-8 facility in Japan.[23] X-rays scattered from the sample were collected via an array of twelve Si analyzer crystals, employing a Si (11 11 11) backscattering setup and a 0.057 nm X-ray wavelength. The Q resolution was set to an approximately 0.92 nm^{-1} full width that was largely independent of Q values between 1.5 and 6.5 nm^{-1}, as determined solely by scattering angles. The full width at half maximum energy resolution ranged from 1.43 to 1.82 meV, depending on the analyzer crystal. Energy scans were performed in conjunction with thermal variations of the lattice constant of the Si backscattering monochromator crystal. A typical energy scan was performed between ±30 meV, which corresponded to a time span of approximately 2 h. Each dataset consisted of two or three scans so as to improve the counting statistics. In order to reduce the scattering background, the sample (contained in a sapphire tube with a 2 mm inner diameter) was set in a vacuum chamber and a vanadium plate with a 0.2 mm aperture was positioned upstream of the sample tube.

2. 4 IXS Data Analysis

The IXS spectrum of each sample was corrected for absorption and the empty cell background, then normalized by the static structure factor, $S(Q)$, obtained by integration of $S(Q, \omega)$ over the energy range in which individual Q values were measured. Each spectrum was expressed as $I(Q, \omega) \propto S(Q, \omega) \otimes R(\omega)$, where $S(Q, \omega)$ and $R(\omega)$ are the dynamical structure factor and the instrumental resolution function, respectively, and the symbol $\otimes$ indicates numerical convolution.

To determine $S(Q, \omega)$ values, we employed a model function consisting of a Lorentzian for the central line and a damped harmonic oscillator (DHO) for two inelastic peaks at positions $\pm\omega_Q$, as expressed by Eq. (1).[24]

$$S(Q,\omega) = \left[\frac{\hbar\omega / k_B T}{1-\exp(-\hbar\omega / k_B T)}\right]\frac{A_0}{\pi}\frac{\Gamma_0}{\Gamma_0^2+\omega^2} + \left[\frac{1}{1-\exp(-\hbar\omega / k_B T)}\right]\times\frac{A_Q}{\pi}\frac{4\omega\Gamma_Q\sqrt{\omega_Q^2-\Gamma_Q^2}}{(\omega^2-\omega_Q^2)^2+4\omega^2\Gamma_Q^2}. \quad (1)$$

Here, A_0 and Γ_0 are the intensity and width of the central peak, respectively, $\hbar$, k_B and T are the Planck constant, the Boltzmann constant and temperature, respectively, while A_Q and Γ_Q are the intensity and width (that is, the damping factor) of the inelastic peaks, respectively. The expression $\hbar\omega/k_BT\ (1 - \exp(-\hbar\omega/k_BT))^{-1}$ represents the Bose factor, which is an asymmetrical weight factor for Stokes and anti-Stokes regions that varies with temperature.

3. Results and Discussion

3. 1 Thermal Conductivity

Table 1 summarizes the thermal conductivity values at 25 and 80°C for nanofluids containing various amounts of Cu NPs. The EG thermal conductivity values at 25 and 80°C were determined to be 0.255 and 0.259 W/m·K, respectively, both of which are very close to the literature values of 0.251 and 0.262 W/m·K, demonstrating the validity of the experimental methodology. As the Cu NP concentration was increased, the thermal conductivity also increased, with a greater rise at 80°C than at 25°C.

As noted, nanofluids based on water with alumina NPs were also assessed, although alumina NPs/EG and Cu NPs/water dispersions were not made, due to the difficulty in obtaining suitable dispersions. The data from these nanofluids are provided in Table 1. The thermal conductivities of water dispersions at 25 and 80°C were estimated to be 0.59 and 0.716, respectively, both of which are quite close to the literature values of 0.606 and 0.6690 W/m·K for pure water. As the case with Cu nanofluids, thermal conductivity increases with increasing the amount of alumina NPs. The thermal conductivities measured at 80°C are also higher than those at 25°C.

The Maxwell-Garnett theory was employed to examine the increase in thermal conductivity, by expressing the rate of increase in the thermal conductivity, k_{nf}/k_b, an in Eq. (2).[25] Here, k_{nf}, k_b and k_p represent the thermal conductivity of the nanofluid, the base liquid and the NPs, while Φ is the NP volume fraction in the dispersion, which is much less than unity.

$$\frac{k_{nf}}{k_b} = \frac{k_p + 2k_b + 2(k_p - k_b)\phi}{k_p + 2k_b - 2(k_p - k_b)\phi}. \quad (2)$$

The experimental thermal conductivity increases at 25 and 80°C are compared to the values calculated using Eq. (2) in **Table 2**. Note that, as the theoretical values at both temperatures were very similar, only the 25°C theoretical data are provided. The specimens with Cu NPs exhibited increase rates greater than the theoretical values at 80°C, demonstrating a significant effect. It is therefore evident that the Cu NPs significantly affected the motion of the solvent molecules.

Conversely, the alumina NPs had little effect on the thermal conductivity, such that 2.5 vol% alumina NPs increased the thermal conductivity only by a factor of 1.08. In addition, the experimental data were all below

Table 1 Effect of NP type and concentration on thermal conductivity of nanofluids.

Exp. No	NPs	Solvent	Concentration [vol%]	25ºC [W/m·K]	80ºC [W/m·K]
TC-EG-1	-	EG	0	0.255	0.259
TC-EG-2	Cu	EG	0.61	0.256	0.270
TC-EG-3	Cu	EG	1.21	0.269	0.283
TC-EG-4	Cu	EG	1.82	0.277	0.296
TC-WA-5	-	water	0	0.590	0.716
TC-WA-6	Al_2O_3	water	2.53	0.635	0.777
TC-WA-7	Al_2O_3	water	7.60	0.758	0.918

Table 2 Thermal conductivity increase for various nanofluids.

Exp. No	NPs	Solvent	Concentration [vol%]	Relative thermal conductivity		
				Theory	25ºC	80ºC
TC-EG-2	Cu	EG	0.61	1.03	1.00	1.04
TC-EG-3	Cu	EG	1.21	1.05	1.06	1.09
TC-EG-4	Cu	EG	1.82	1.08	1.09	1.14
TC-WA-6	Al_2O_3	water	2.53	1.10	1.08	1.09
TC-WA-7	Al_2O_3	water	7.60	1.34	1.29	1.28

the theoretical predictions, showing that the motion of the water molecules was only minimally impacted by these NPs. The alumina NPs were approximately 30 nm in size, and thus smaller than the 60 nm Cu NPs, but still on the same order of magnitude. Therefore, the size difference is likely not a factor in the variations in the results. However, alumina is an insulator whereas Cu is a metal, which could affect the interactions of the NPs with polar solvent molecules.

3. 2 IXS

Table 3 presents the IXS data acquired from the samples. Specimens having lower densities were selected for these trials, as the high degree of elastic scattering from the Cu NPs may otherwise have complicated the assessments. In each case, the dynamic structure factor, S (Q, ω), was determined upon subtracting the background scattering values for an empty cell. The normalized IXS spectrum of sample EG-3 (spectrum IXS-EG-3), obtained at Q = 5.58 nm^{-1}, is presented in **Fig. 1**. Quasi-elastic scattering is evident in the vicinity of 0 meV, along with a shoulder at 4.7 meV indicative of inelastic excitation. Cu NPs would be expected to generate peaks at significantly higher energies than the solvent, and the DHO method was employed to separate this shoulder peak from the primary quasi-elastic scattering peak. For each sample, 24 datasets acquired at different Q values were assessed to obtain the inelastic excitation energy values. **Figure 2** provides the IXS spectra obtained for IXS-EG-3 at different Q values.

The excitation energy values are plotted against Q in **Fig. 3**. The slope of the best linear fit to these data was used to find the high-frequency sound velocity (HFSV), giving a value of 2.56 km/s. The estimated EG HFSV value is 2.31 km/s, and so the HFSV increased by a factor of 1.11 due to the Cu NPs. The estimated HFSV of EG is 1.4 times greater than the sound velocity of EG (1.67 km/s). The HFSV for an organic solvent or for water will typically be greater by a factor of 1.3 or 2, respectively, compared to the sound velocity. The presence of multiple hydroxyl groups in the EG molecules increases its sound velocity somewhat compared to those of other organic solvents.

The HFSV values for each specimen are provided in Table 3, from which it is evident that HFSV increases along with the concentration of Cu or alumina NPs. This trend suggests that the collective dynamics of EG or water were modified by the NPs. In the case of Cu NPs, even small amounts affected the movement of EG molecules, while the addition of alumina to water had a lesser effect.

Table 4 provides values obtained by dividing the sound velocity increase ratio by the volume-based concentration. These data show that the Cu NPs were at least ten times more effective compared to alumina, keeping in mind that different solvents were used. The Cu NPs evidently had a very pronounced impact on the sound velocity.

Table 3 High-frequency sound velocities in nanofluids.

Exp. No	NPs	Solvent	Concentration [vol%]	25ºC [km/s]
IXS-EG-1	-	EG	0	2.31 ± 0.01
IXS-EG-2	Cu	EG	0.5	2.34 ± 0.02
IXS-EG-3	Cu	EG	1.32	2.56 ± 0.03
IXS-WA-4	-	water	0	2.72 ± 0.03
IXS-WA-5	Al_2O_3	water	2.53	2.76 ± 0.02
IXS-WA-6	Al_2O_3	water	7.60	2.84 ± 0.03

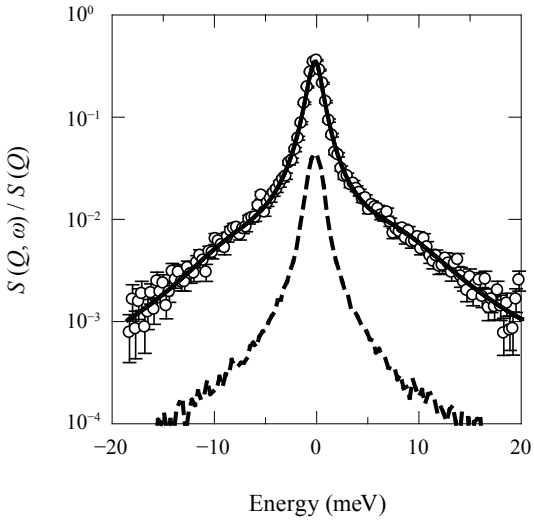

Fig. 1 Normalized inelastic X-ray scattering spectrum (trial IXS-EG-3, acquired at Q = 5.58 nm^{-1}). The solid line represents the DHO and Lorentzian fit (Eq. (1)), including convolution of the resolution function (broken line).

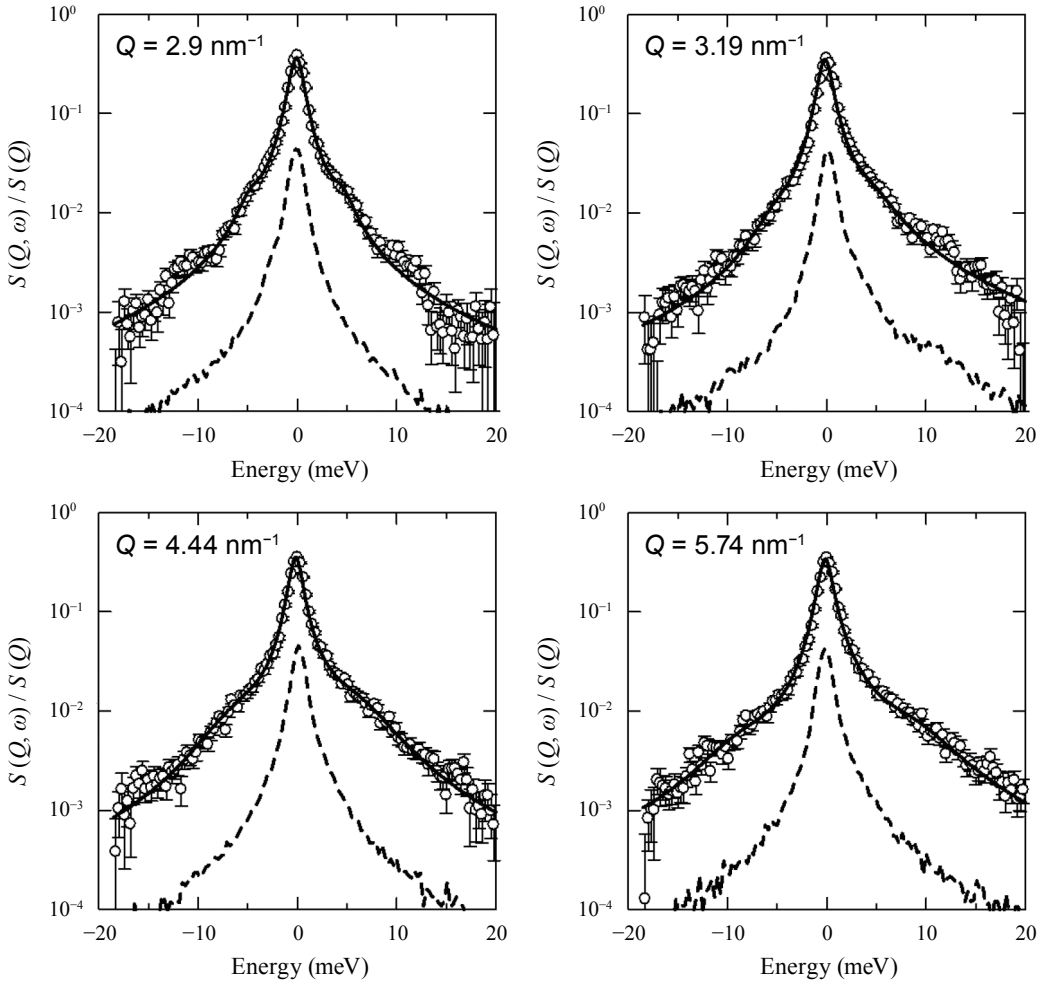

Fig. 2 Normalized inelastic X-ray scattering spectra of IXS-EG-3 at different Q values. The solid line represents the DHO and Lorentzian fit including convolution of the resolution function (broken line).

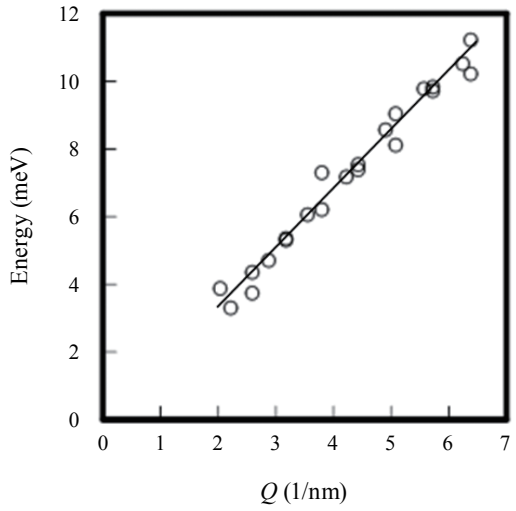

Fig. 3 Inelastic excitation energy (from IXS-EG-3 trials) as function of Q. The solid line represents a least squares fit.

Table 4 Effect of NP type and concentration on high-frequency sound velocity in the nanofluids.

Exp. No	NPs	Solvent	Concentration [vol%]	Relative HFSV	Increase rate/conc.
IXS-EG-2	Cu	EG	0.5	1.01 ± 0.01	2.60
IXS-EG-3	Cu	EG	1.32	1.11 ± 0.01	8.41
IXS-WA-5	Al_2O_3	water	2.53	1.01 ± 0.01	0.49
IXS-WA-6	Al_2O_3	water	7.60	1.02 ± 0.01	0.50

4. Conclusions

Thermal conductivity data were acquired from nanofluids composed of alumina NPs in water and Cu NPs in EG. The thermal conductivity was found to increase along with the Cu NP concentration and the extent of this increase was greater than that predicted by the Maxwell-Garnett theory. Cu NPs evidently modify the motion of solvent molecules to a significant degree. Conversely, alumina NPs in water produce thermal conductivity values equal to or below the theoretical values.

IXS data were used to determine the HFSV values for the nanofluids. This allowed an examination of the effects of NPs on heat transfer and molecular dynamics in these liquids, as both structural relaxation and thermal conductivity are reflected in the HFSV. Low concentrations of Cu NPs increased the HFSV by a factor of 1.11, and so the EG collective dynamics seem to have been affected. The addition of alumina NPs had a minimal effect, which highlights the greater impact of the Cu NPs. These results demonstrate that IXS is a viable means of assessing the effects of NPs on various liquid media, and could assist in the future design of high-efficiency nanofluids.

Acknowledgements

The authors thank Dr. Yoshiaki Fukushima and Dr. Kazuya Kamazawa of CROSS, Prof. Toshio Yamaguchi of Fukuoka University, Dr. Hiroshi Uchiyama, Dr. Satoshi Tsutsui of JASRI SPring-8, and Dr. Alfred Q. R. Baron of RIKEN for fruitful discussion and cooperating with the experiments.

References

(1) Eastman, J. A., Choi, S. U. S., Li, S., Yu, W. and Thompson, L. J., "Anomalously Increased Effective Thermal Conductivities of Ethylene Glycol-based Nanofluids Containing Copper Nanoparticles", *Appl. Phys. Lett.*, Vol. 78, No. 6 (2001), pp. 718-720.

(2) Patel, H. E., Das, S. K., Sundararajan, T., Nair, A. S., George, B. and Pradeep, T., "Thermal Conductivities of Naked and Monolayer Protected Metal Nanoparticle Based Nanofluids: Manifestation of Anomalous Enhancement and Chemical Effects", *Appl. Phys. Lett.*, Vol. 83, No. 14 (2003), pp. 2931-2933.

(3) Yu, W., Xie, H., Chen, L. and Li, Y., "Investigation on the Thermal Transport Properties of Ethylene Glycol-based Nanofluids Containing Copper Nanoparticles", *Powder Technol.*, Vol. 197, No. 3 (2010), pp. 218-221.

(4) Liu, M.-S., Lin, M. C.-C., Tsai, C. Y. and Wang, C.-C., "Enhancement of Thermal Conductivity with Cu for Nanofluids Using Chemical Reduction Method", *Int. J. Heat Mass Transfer*, Vol. 49, No. 17-18 (2006), pp. 3028-3033.

(5) Li, X. F., Zhu, D. S., Wang, X. J., Wang, N., Gao, J. W. and Li, H., "Thermal Conductivity Enhancement Dependent pH and Chemical Surfactant for Cu-H_2O Nanofluids", *Thermochim. Acta*, Vol. 469, No. 1-2 (2008), pp. 98-103.

(6) Kole, M. and Dey, T. K., "Enhanced Thermophysical Properties of Copper Nanoparticles Dispersed in Gear Oil", *Appl. Therm. Eng.*, Vol. 56, No. 1-2 (2013), pp. 45-53.

(7) Amiri, M., Movahedirad, S. and Manteghi, F., "Thermal Conductivity of Water and Ethylene Glycol Nanofluids Containing New Modified Surface SiO_2-Cu Nanoparticles: Experimental and Modeling", *Appl. Therm. Eng.*, Vol. 108 (2016), pp. 48-53.

(8) Garg, J., Poudel, B., Chiesa, M., Gordon, J. B., Ma, J. J., Wang, J. B., Ren, Z. F., Kang, Y. T., Ohtani, H., Nanda, J., McKinley, G. H. and Chen, G., "Enhanced Thermal Conductivity and Viscosity of Copper Nanoparticles in Ethylene Glycol Nanofluids", *J. Appl. Phys.*, Vol. 103, No. 7 (2008), 074301.

(9) Keblinski, P., Phillpot, S. R., Choi, S. U. S. and Eastman, J. A., "Mechanisms of Heat Flow in Suspensions of Nano-sized Particles (Nanofluids)", *Int. J. Heat Mass Transfer*, Vol. 45, No. 4 (2002), pp. 855-863 .

(10) Gao, J. W., Zheng, R. T., Ohtani, H., Zhu, D. S. and Chen, G., "Experimental Investigation of Heat Conduction Mechanisms in Nanofluids. Clue on Clustering", *Nano Lett.*, Vol. 9, No. 12 (2009), pp. 4128-4132.

(11) Bencivenga, F., Cunsolo, A., Krisch, M., Monaco, G., Ruocco, G. and Sette, F., "High-frequency Dynamics of Liquid and Supercritical Water", *Phys. Rev. E*, Vol. 75, No. 5 (2007), 051202.

(12) Yamaguchi, T., Yoshida, K., Yamamoto, N., Hosokawa, S., Inui, M., Baron, A. Q. R. and Tsutsui, S., "Collective Dynamics of Supercritical Water", *J. Phys. Chem. Solids*, Vol. 66, No. 12 (2005), pp. 2246-2249.

(13) Kamiyama, T., Hosokawa, S., Baron, A. Q. R., Tsutsui, S., Yoshida, K., Pilgrim, W.-C., Kiyanagi, Y. and Yamaguchi, T., "Acoustic Phonon Dynamics in Liquid CCl_4", *J. Phys. Soc. Jpn.*, Vol. 73, No. 7 (2004), pp. 1615-1618.

(14) Yoshida, K., Yamamoto, N., Hosokawa, S., Baron, A. Q. R. and Yamaguchi, T., "Collective Dynamics of Sub- and Supercritical Methanol by Inelastic X-ray Scattering", *Chem. Phys. Lett.*, Vol. 440, No. 4-6 (2007), pp. 210-214.
(15) Hosokawa, S., Inui, M., Kajihara, Y., Matsuda, K., Ichitsubo, T., Pilgrim, W.-C., Sinn, H., González, L. E., González, D. J., Tsutsui, S. and Baron, A. Q. R., "Transverse Acoustic Excitations in Liquid Ga", *Phys. Rev. Lett.*, Vol. 102, No. 10 (2009), 105502.
(16) Kajihara, Y., Inui, M., Hosokawa, S., Matsuda, K. and Baron, A. Q. R., "Dynamical Inhomogeneity of Liquid Te Near the Melting Temperature Proved by Inelastic X-ray Scattering Measurements", *J. Phys.: Condens. Matter*, Vol. 20, No. 49 (2008), 494244.
(17) Inui, M., Hosokawa, S., Matsuda, K., Tsutsui, S. and Baron, A. Q. R., "Heavy Particle Dynamics in Liquid Se: Inelastic X-ray Scattering", *J. Phys. Soc. Jpn.*, Vol. 76, No. 5 (2007), 053601.
(18) Fievet, F., Lagier, J. P., Blin, B., Beaudion, B. and Figlarz, M., "Homogeneous and Heterogeneous Nucleations in the Polyol Process for the Preparation of Micron and Submicron Size Metal Particles", *Solid State Ionics*, Vol. 32-33, Part 1 (1989), pp. 198-205.
(19) Toshima, N. and Wang, Y., "Novel Preparation, Characterization and Catalytic Properties of Polymer-protected Cu/Pd Bimetallic Colloid", *Chem. Lett.*, Vol. 22, No. 9 (1993), pp. 1611-1614.
(20) Ishizaki, T. and Watanabe, R., "A New One-pot Method for the Synthesis of Cu Nanoparticles for Low Temperature Bonding", *J. Mater. Chem.*, Vol. 22, No. 48 (2012), pp. 25198-25206.
(21) Ishizaki, T., Usui, M. and Yamada, Y., "Thermal Cycle Reliability of Cu-nanoparticle Joint", *Microelectron. Reliab.*, Vol. 55, No. 9-10 (2015), pp. 1861-1866.
(22) Saterlie, M., Sahin, H., Kavlicoglu, B., Liu, Y. and Graeve, O., "Particle Size Effects in the Thermal Conductivity Enhancement of Copper-based Nanofluids", *Nanoscale Res. Lett.*, Vol. 6, No. 1 (2011), Article No. 217.
(23) Baron, A. Q. R., Tanaka, Y., Goto, S., Takeshita, K., Matsushita, T. and Ishikawa, T., "An X-ray Scattering Beamline for Studying Dynamics", *J. Phys. Chem. Solids*, Vol. 61, No. 3 (2000), pp. 461-465.
(24) Fåk, B. and Dorner, B., "Phonon Line Shapes and Excitation Energies", *Phys. B: Condens. Matter*, Vol. 234-236 (1997), pp. 1107-1108.
(25) Wang, X.-Q. and Mujumdar, A. S., "Heat Transfer Characteristics of Nanofluids: A Review", *Int. J. Therm. Sci.*, Vol. 46, No. 1 (2007), pp. 1-19.

Figs. 1-3 and Tables 1-4
Reprinted from J. Molecular Liquids, Vol. 248 (2017), pp. 468-472, Yano, K., Yoshida, K., Kamazawa, K., Uchiyama, H., Tsutsui, S., Baron, A. Q. R., Fukushima, Y. and Yamaguchi, T., Investigation of Collective Dynamics of Solvent Molecules in Nanofluids by Inelastic X-ray Scattering, © 2017 Elsevier, with permission from Elsevier.

Kazuhisa Yano
Research Fields:
- Nanoporous Materials
- Nanocomposites
- Phonon Study

Academic Degree: Dr.Eng.
Academic Society:
- The Chemical Society of Japan

Koji Yoshida*
Research Field:
- Solution Chemistry

Academic Degree: Dr.Eng.
Academic Societies:
- The Chemical Society of Japan
- The Japanese Society for Neutron Science
- The Japan Society of High Pressure Science and Technology

*Fukuoka University

